Advances in Ionospheric Propagation Modelling at High-Latitudes

S.E. Ritchie*†, F. Honary. †

*Commission for Communications Regulation (ComReg), Irish Life Centre,
Lower Abbey Street, Dublin 2, Ireland
Email: s.ritchie@lancaster.ac.uk

†Department of Communication Systems, University of Lancaster,
Lancaster, LA1 4W4, UK
Email: f.honary@lancaster.ac.uk

Keywords: Ionosphere, High-latitude, Modelling.

Abstract

Many services rely on the output of propagation planning tools to predict the future state of the ionosphere and the availability of suitable communications channels. While this approach is adequate for services operating at high-latitudes during quiet ionospheric conditions it is insufficient to deal with a disturbed ionosphere. This paper presents the results of empirical modelling of the changes that occur in the D- and E-regions of the ionosphere following the onset of disturbed conditions as defined by the occurrence of a storm sudden commencement.

1 Introduction

The use of HF communications at high latitudes still forms the back bone of many communications systems. At high latitudes there are few alternatives to HF radio for the merchant and fishing fleets, military forces (land, sea and air) and for the civil aviation industry. The typical features of HF radio communications following magnetic disturbances include: the incidence of large absorption spikes, changes in propagation modes, reductions in operational frequencies as electron density in the F-region changes and a growth in auroral absorption. Ionospheric propagation during magnetic disturbances at these latitudes has been an enigma, in part because ionograms do not always provide analysable data due to absorption, blanketing and spread-F effects.

Numerous studies of the high-latitude ionosphere have been undertaken to aid in understanding the response of the HF communication channel to space weather effects. A review of both effects and the associated problems, with many references, is provided in [1, 2, 3, 4] and [5]. More recently the impact of 14 geomagnetic storms, which occurred during 1997-1999, on radio propagation conditions, was examined [6].

1.1 HF Propagation Prediction.

The validity of using HF propagation prediction programs has been addressed [7] and good agreement between the prediction and measurements made during quiet conditions has been found. It has also been noted the aggregate correct prediction of these programs was only ~ 45% under disturbed conditions [5].

The use of propagation prediction programs to establish, in advance, the choice of operating frequency is still the basis of operations of many communication systems. For example HF broadcasting requires frequencies and schedules to be agreed months in advance of actual usage and military exercises at high-latitudes are preceded by detailed advance planning and the distribution of set tables of frequencies well in advance. It appears that this methodology of advance planning and the range of hourly median parameters produced by the propagation prediction programs is adequate for operational purposes, during quiet conditions. The problem to be overcome is to determine what propagation parameters need to be modified during disturbed conditions, that is, what consequential modifications need to be made to the communications system parameters to ensure some form of continued operation during disturbed conditions.

From an operational point of view a technique is needed to address the uncertainties generated by ionospheric disturbances on key ionospheric parameters and a number of authors have examined this problem (e.g. [8, 9, 10 and 11]). A number of authors have also proposed the use of oblique and vertical sounding data to provide near real-time ionospheric maps and communication performance parameters; e.g. [12 and 13]. Certainly while each of these approaches has different applications and merits, the authors have chosen another approach.

The authors' approach is that advocated by Lundborg et al [14] – "It seems that priority should be given to the

development of *propagation prediction*[1] methods which predict the deviation from the median rather than the median".

What is missing is the defining point at which the deviation from the median starts. The authors have used the storm sudden commencement (SSC) as this defining point.

1.2 Storm Sudden Commencement.

Coronal mass ejections from the Sun give raise to shock waves in the solar wind. The related pressure pulses, when impinging on the earth's magnetosphere, both compress it and increase the magnetopause current. This leads into a few tens of nano-Tesla (nT) change in the low-latitude ground-based magnetic field intensity, lasting typically for some tens of minutes. These signatures are called Storm Sudden Commencements (SSC) and announce the onset of geomagnetic storm and subsequently identify the start of a period of change in composition of the ionosphere, such as reconfiguration of the magnetosphere, injection of particles into the radiation belts, changes of particle drift velocities, sudden onsets of wave activities etc.

The advantages of using SSC events as the point of origin is two fold. Firstly, the occurrence and timing of an SSC is internationally agreed [15] and therefore a very useful reference point when comparing results from a number of different instruments in different locations. Secondly, the SSC identifies the start of the change of composition of the ionosphere with associated energetic particle precipitation – that is the transition point between a 'quiet' and a 'disturbed' ionosphere.

2 Modelling Changes in the D-region

The first manifestation, coincident with the SSC is a large absorption spike, known as sudden commencement absorption (SCA), lasting tens of minutes that disrupts low to mid HF frequency operations. The cause of this affect is the sudden increase of electron density in the D-layer due to deeply penetrating charged particles [16].

In a recent paper [17] the authors set out to find the best predictor of SCA based on solar wind parameters. The authors examined the characteristics of SCA across more than half a solar cycle, from the sunspot maximum in 2000 to the near sunspot minimum in 2006. Having discounted ambiguous events, 175 SSC events and the co-incident SCA were investigated.

2.1 Data.

For each of the 175 events data from the IRIS Riometer at Kilpisjärvi (69.10N, 20.80E, L=6.06) was used to measure the peak absorption resulting from particle precipitation caused by SSC shocks. In essence a riometer observes temporal variations in ionisation in the D and E regions caused by charged particle precipitation [18]. An example of such an absorption signature following a SSC event at 14:10 UT on 3 April 2004, is shown in figure 1.

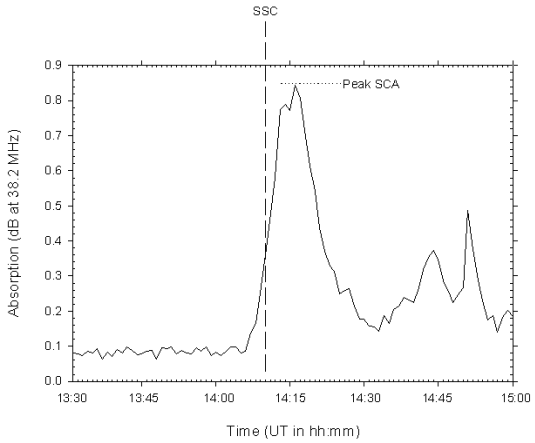

Figure 1: Riometer measurement from the central beam of the IRIS riometer - 1 minute resolution sampling. The SSC occurred at 14:10 UT which is indicated by the long-dashed line. The peak SCA measured in this example is indicated by the dotted line.

Before the SSC the absorption was negligible. At the start of the SSC the absorption increases within 5 minutes to 0.8 dB, peaking at 0.85 dB ten minutes after the SSC event commences. Fifteen minutes after the peak the absorption falls to less than 0.2 dB with some variability thereafter due to subsequent magnetospheric activity.

Solar wind and IMF Data for this study was sourced from measurements taken by the ACE spacecraft. See [19] for details of the satellite and instrumentation. For each SSC event the following solar wind parameters were measured before and after the SSC:

- B – the IMF field strength (nT)
- B_z – the magnitude and direction of the B_z component of the solar wind (nT)
- V_p - solar wind proton velocity ($km.s^{-1}$)
- N_p – solar wind proton density (cm^{-3})

2.2 Results.

As the data spans more than half a solar cycle it was possible to determine if solar activity influenced the data set. This was done by evaluating the link between SCA and the change in IMF magnitude against solar activity as reflected by the value of the relevant monthly sunspot number. Across a range of monthly sunspot number from 8 to 170 it was concluded that that there is no causal link between SCA and sunspot number or between IMF magnitude and SCA, other than in the frequency of occurrence of SSC events. This last point is not unexpected as higher sunspot levels reflect the increase in the

[1] The italic text has been inserted by the authors to clarify the context of the quote

number of active regions on the sun that are the source of shocks leading to SSC events.

Having calculated and compared the median, median and standard deviation of SCA between the day (6-18 MLT) and the night (18-6 MLT) it was shown that while the occurrence of SCA is slightly greater during the day there is no significant difference in the mean, median or standard deviation values of SCA between night and day.

For all events where B_z information was available (152 events) the mean, median and standard deviation of SCA for all the possible B_z movements (e.g. north to south, north to further north, etc) were compared against each other. The similarity in statistics between all four types of event indicates that the direction of B_z has little impact on the typical values of SCA, for example, more than half of the selected SCA events occurred during northward B_z movements, which in some cases continued even more strongly northward after the SSC event.

2.2 Modelling of SCA

Having determined that there is no causal link between SCA and sunspot number, no causal link between IMF magnitude and SCA, no significant difference in night time and day time SCA and that B_z has little impact on the typical values of SCA the best predicator of SCA was sought. The method used was to find the best predictor of SCA based on one or more solar wind parameters in order to clarify the affect of solar wind and IMF shocks on SCA. In order to do this a substantial body of work was undertaken to correlate each of the parameters B, B_z, V_p and N_p with the absolute, average and median values of SCA measured at the moment of SSC.

The best results were achieved when using the median value of measured SCA. The median value is a measure of central tendency that provides us with a description of the entire data set and is especially useful when data sets contain a few extremely high values that can skew the distribution, as is the case here. The median is less sensitive to extreme values and is an appropriate measure when dealing with the highly variable ionosphere and magnetosphere. It is for similar reasons and also convenient that hourly median values are the standard output from HF propagation prediction programmes and using median values of SCA allows comparisons to be made against predicted median values of absorption.

Figure 2 consists of four panels showing the median value of SCA compared against the step change in IMF and solar wind parameters at the moment of SSC; (ΔB) (top panel), solar wind velocity (ΔV_p) (second panel) and solar wind particle density (ΔN_p) (bottom panel). A first order regression is applied to the last scatter plot and a second order regression is applied to the first two scatter plots. The choice of only a first order regression for the last plot was determined by the wide spread of values in the data. Figure 2 demonstrates the strong correlation between solar wind velocity and SCA but also the even stronger correlation between the IMF and SCA.

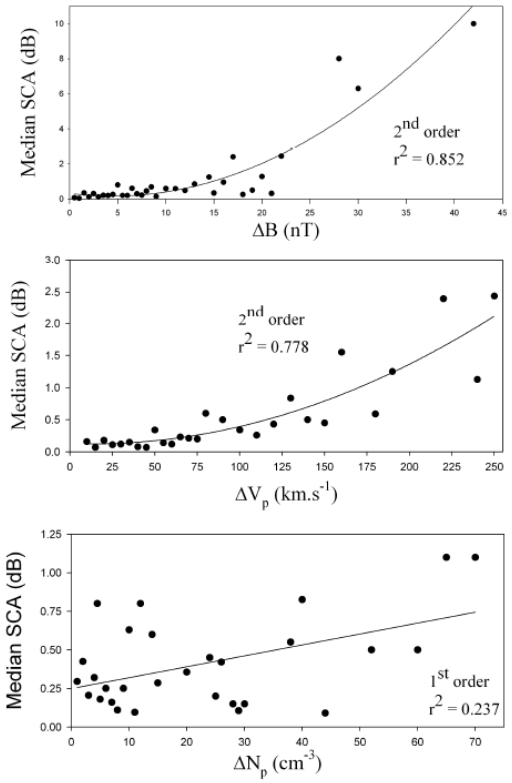

Figure 2: Scatter plot and regression of median SCA vs. (from top to bottom) ΔB, ΔV_p and ΔN_p

By a wide margin, the strongest correlation was found between the median value of SCA measured and ΔB, the step change in IMF magnitude that occurred during the shock. The fitted curve in the top panel of figure 2, with a correlation coefficient (R^2) of 0.852, is a second order equation of the form:

$$A_m = \quad - \quad \Delta \; + \quad \Delta \; ^{\wedge}$$

Where: Am = the median value of SCA expected
ΔB = the change in IMF due to the shock

The fit for ΔB against median SCA is very good at values of ΔB < 25 nT, reducing somewhat at values of ΔB > 25 nT. While this does bear further investigation less than 3% of SSC shocks in the data, that is ~ 5 events in a six year period generate a change in IMF magnitude greater than 25 nT.

This result has a direct application to real-time and near-time ionospheric propagation prediction in respect of the predicted change in median value of absorption following a disturbance the D-region.

3 Modelling Changes in the E-region

Sporadic-E (E_s) is a problem in high latitude HF communications because of its irregular and as yet unpredictable behaviour. E_s has different characteristics in different latitudinal zones and there may be several mechanisms governing the behaviour of these layers. The high latitude E_s layers are generally considered to be due to particle precipitation [20, 21, 22, 23]. It has been found that electron precipitation usually is the major cause for the formation of the high latitude sporadic E-layer and that the modified wind shear mechanism, which takes into account the effect of electric fields, is important under low electron precipitation conditions only, i.e. 'quiet' conditions [24].

In the three to five hours following the onset of geomagnetic activity the ionospheric path is characterised by changes in the mode of propagation. This is caused by an enhanced sporadic-E layer overshadowing the usual F-layer propagation paths [25]. These sporadic-E paths are known to be able to support HF communications during ionospheric storm periods and this section presents the results of research that has empirically modelled the deviations from the predicated median of f_0E_s following the onset of an ionospheric storm and provides guidance to HF communications operators for maintaining link establishment.

3.1 Data.

The data used in this section is gathered from f-plots generated at the Sodankylä observatory which is located 120 km north of the Arctic Circle in Finland, 67° 22′ N, 26° 38′ E, L-value 5.2. Data for this research work was gathered over six years from the sunspot minimum in 2000 until the near sunspot maximum in 2006.

The f-plot is a daily graph of the frequency characteristics of all the daily ionograms as a function of time, using an internationally agreed convention, so that detailed observations from different stations may be compared efficiently. The f-plot provides a summary of the original observations with the minimum of interpretation and enables difficult decisions needed for hourly tabulations to be made with due consideration of all the available data. This is particularly important at high latitude stations were blackouts, spread echoes or rapidly changing oblique reflections frequently prevent the normal characteristics from being observed on individual hourly ionogram records. Figure 3 is an example of an f-plot used in this analysis.

It has been acknowledged that the f-plot is a valuable tool for identifying variations in the ionosphere, in the interpretation of complex records, particularly at high latitudes and it has become a primary tool for analysing the hour-to-hour or day-to-day changes in the ionosphere [26].

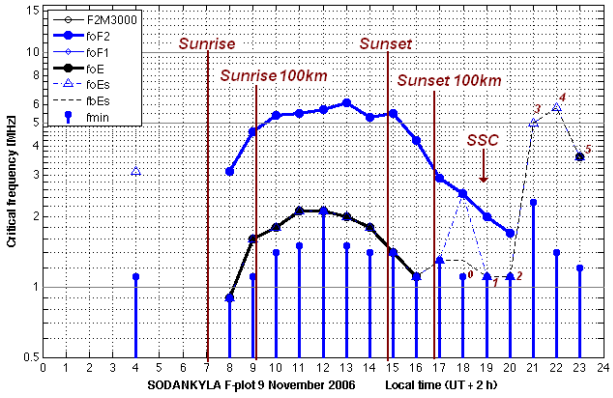

Figure 3: Example of an f-plot - the arrow at 18:50 MLT indicates the occurrence time of the SSC.

The starting point for this study is again the occurrence of an SSC indicating the occurrence of magnetospheric changes and modifications to the ionosphere – that is the onset of a disturbed state. In order to collect data that captures all the E-layer effects which are initiated with a SSC occurring, data is collected for the four hours following SSC. In order to accumulate an adequate number of samples the day was split into four sectors. Sector A covering the period 0-6 MLT, sector B covering 6-12 MLT, sector C covering 12-18 MLT and sector D covering 18-24 MLT.

For each of the four hours following an SSC, the following statistics are collected for each sector from the f-plot: The mean, median, minimum, maximum, lower quartile and upper quartile of the change in critical frequency (Δf_oE) that occurs in each sector as well as the onset of screening (total blanketing) that occurs in each sector.

The difference in critical frequency measured on each hour following an SSC event is used to define the variability that occurs. This difference is designated in this paper as Δf_oE_{n-m} where Δf_oE is the change in hourly E-layer critical frequency and n and m indicate which hour following the SSC is being measured. These values reflect the reduction or increase in E-layer ionisation due to all applicable factors. However as enhanced ionisation due to particle precipitation which is by far the dominant ionisation source, Δf_oE_{n-m} captures predominantly the influence of particle precipitation.

3.2 Results.

This section examines the variability of E_s in the four hours following an SSC as well as the occurrence of screening. Polar plots are used in figure 4 where the radial axis is Δf_oE and the clock hours indicate local time. The solid dots indicate where full screening of the F layers occurred. The associated line, scatter and error bar plot shows the mean (diamond) and median (circles) values of Δf_oE_{m-n} per sector, the 25% and 75% percentiles between vertical error bars and the count of events in the lower panel.

The statistics show considerable variation, as is expected when working with the ionosphere in general and which is amplified when dealing with the high-latitude ionosphere. A number of significant points are noted from examining the plots of figure 4. It is noted that $\Delta f_oE_{0\text{-}1}$ can be positive and negative, this depends on whether or not storm induced precipitation has commenced in this hour or not. Full blanketing (screening) can occur even when $\Delta f_oE_{0\text{-}1}$ is negative. This implies that the F-layer ionisation has dramatically reduced so even though the E-layer might be penetrated, no F-layer reflecting plane exists. Screening can occur when $\Delta f_oE_{0\text{-}1}$ is zero and this implies that F-layer ionisation is severely reduced or particle precipitation is maintaining a thick highly ionised E_s-layer.

In the first hour following SSC when $\Delta f_oE_{0\text{-}1}$ exceeds 2.1 MHz the onset of screening is guaranteed. Screening occurs in all sectors in the first hour ($\Delta f_oE_{0\text{-}1}$) except between 6 – 12 MLT (Sector B) where only one out of 33 events over a six year period caused screening in the first hour. Screening occurs extensively in the second hour when $\Delta f_oE_{1\text{-}2}$ exceeds 1 MHz and exclusively when $\Delta f_oE_{1\text{-}2}$ exceeds 2.1 MHz, identical to what occurs in the first hour ($\Delta f_oE_{0\text{-}1}$).

In the third hour $\Delta f_oE_{2\text{-}3} \approx 2.1$ MHz continues to be a milestone indicator that guarantees screening will occur, with only one exception occurring in six years of data. The extensive occurrence of screening greatly increases in the third hour when $\Delta f_oE_{2\text{-}3}$ exceeds 0.5 MHz which is significantly less than in previous hours.

In the fourth hour $\Delta f_oE_{3\text{-}4} \approx 3$ MHz is now a new milestone indicator that guarantees screening will occur. The extensive occurrence of screening at negative values of $\Delta f_oE_{3\text{-}4}$ in the fourth hour indicates that F-layer ionisation has dramatically reduced and that there is no F-layer reflecting plane even if the E-layer is penetrated. In this hour a $\Delta f_oE_{3\text{-}4} \approx 2.1$ MHz again provides a good threshold with screening occurring exclusively in sectors C and D above this level.

Ring currents during magnetic storms move the auroral region (at the pole ward boundary of the trapping region toward the equator. All field lines from the auroral zone touch the outer boundary of the magnetosphere, thus allowing particle injection. This explains the highest Δf_oE_m-n values that occur in sector D (18-24MLT) as sector D is when the field lines are open to direct particle injection, directly opposite to sector B (9-12 MLT). Sector A and Sector C have similar statistics and variance reflecting their intermediate position between sector D and sector B.

It can be seen from figure 4 that E_s often fully screens the F-layer leaving the operator little choice but to rely on E_s layer reflections instead of F-layer reflections. Noting the sector in which a SSC occurs allows the operator, using the information in figure 4, to modify the operating frequency established by standard prediction methodologies to compensate for the change brought on by ionospheric disturbances to the E-region.

4 Conclusion

HF radiocommunications is still an essential service at high latitudes even though the HF channel is adversely affected by the impact of space weather. Hence the importance of advancing the prediction of propagation during disturbed periods.

Using the occurrence of SSC as the defining point of the transition between a ‘quiet’ and ‘disturbed’ ionosphere ensures a well defined and understood starting point from which to both gather data and predict the deviation of critical ionospheric parameters from the expected norm following the onset of disturbances.

The first manifestation of an ionospheric disturbance is a large absorption spike lasting tens of minutes that disrupts low to mid HF frequency operations. The cause of this affect is the sudden increase of electron density in the D-layer due to deeply penetrating charged particles. Research has demonstrated that the amplitude of the expected absorption spike can be empirically determined based on IMF data. Depending on solar wind velocity, this data is available 30 – 60 minutes before the observed step-change in IMF propagates to the earth’s magnetosphere.

The second manifestation of an ionospheric disturbance dealt with in this paper is the formation of intense and prolonged $E_{s.}$ Sporadic-E layers are important to consider at high latitudes where they modify the mode of propagation and often totally screen the f-layer off. An investigation into disturbances affecting the E-region has lead to the characterisation of the change in the median value of the critical frequency of E_s and the occurrence of fully-blanketing E_s follow the onset of disturbances The results detail the deviation of f_oE_s (from its quiet ionosphere value) for the four hours immediately following the SSC.

The approach adopted in this research is to empirically predict the deviation of key ionospheric parameters (absorption, f_0E and the occurrence of E-layer screening) from the median value as predicated by standard propagation prediction methodologies. The strength of this approach is that system operators can adjust for the deviation of critical frequencies from the quiet-ionosphere predictive norm without the need for a supporting network of vertical and/or oblique sounders.

Acknowledgements

Riometer data originated from the Imaging Riometer for Ionospheric Studies (IRIS), operated by the Department of Communications Systems at Lancaster University (UK) in collaboration with the Sodankylä Geophysical Observatory, and funded by the Science and Technology Facilities Council (STFC)

I acknowledge the Sodankylä Geophysical Observatory, Finland for use of the f-plot data.

References

[1] F. Leid, "High frequency radio communications with emphasis on polar problems", AGARDograph 104, Technivision, Maidenhead, UK (1967)

[2] J.M. Goodman, "HF Communications: Science and Technology", Van Nostrand Reinhold, New York (1991).

[3] K. Davies, "Ionospheric Radio", IEE Electromagnetic Wave Series, Vol 31, Peter Peregrinus Ltd, Institute of Engineers, London, 1990.

[4] R.D. Hunsucker, and H.F. Bates, "Survey of polar and auroral region effects on HF propagation", *Radio Science*, **4**, No. 4, 347-365 (1969)

[5] R.D. Hunsucker, and J.K. Hargreaves, "The high latitude ionosphere and its effects on radio propagation", Cambridge University Press (2003)

[6] D.V. Blagoveshchensky, A.S. Kalishin and M.A. Sergeeva, "Space weather effects on radio propagation: Study of the CEDAR, GEM and ISTP storm events", *Annales Geophysicae*, **26**, 1479-1490 (2008)

[7] M. Bröms and B. Lundborg, "Results from Swedish oblique sounding campaigns", *Annali di Geofisica*, **XXXVII**, N.2 (1994)

[8] R.I. Barnes, R. S. Gardiner-Garden and T. J. Harris, "Real time ionospheric models for the Australian Defence Force", *Proceedings of a Workshop on the Applications of Radio Science*, La Trobe University, 27-29 April (2000).

[9] R.J. Norman, I.G. Platt, P.S. Cannon, "A HF ionospheric propagation model using analytic ray tracing", *IEE Colloquium on HF Antennas and Propagation*, pp. 8/1 – 8/6, 14 Nov (1995)

[10] I. Tsagouri, Zolesi, B., Belehaki, A., and Cander, L.R. "Evaluation of the performance of the real-time updated simplified ionospheric regional model for the European area.", Journal of Atmospheric and Solar-Terrestrial Physics, 67, 1137-1146 (2005).

[11] R. Gardiner-Garden, A. Heitmann, B. Northey and M. Turley, "Modelling uncertainty in a real-time model (nowcast) of the ionosphere", *12th International Ionospheric Effects Symposium*, IES2008, 13-15 May (2008)

[12] B.Zolesi, Belehaki, A., Tsagouri, I., and Cander, L.R. "Real-time updating of the Simplified Ionospheric Regional Model for operational applications", *Radio Science*, **39**, 2, (2004).

[13] J.M Goodman, and J.W. Ballard, "Dynamic management of HF communication and broadcasting systems", *IEE Colloquium on Frequency Selection and Management Techniques for HF Communications,* pp 18/1 – 18/05 (1999)

[14] B. Lundborg, M. Bröms and H. Derblom, "Oblique sounding of an auroral ionospheric HF channel", *Journal of Atmospheric and Terrestrial Physics*, **57**, No 1, 51 – 63 (1995)

[15] ISGI, "Service International des Indices Geomagnetiques", *Bureau des publications du SIIG*, http://isgi.cetp.ipsl.fr/lesdonne.htm, 23 March (2008)

[16] T. Kikuchi, H. Yamagishi, "Latitudinal features of cosmic noise absorption at the time of SSC-triggered substorm a observed with scanning beam riometer", *Proceedings of the NIPR symposium on upper atmospheric physics*, **2**, 9-14 (1989)

[17] S.E. Ritchie, and F. Honary, "Observed characteristics of sudden commencement absorption", *Journal of Atmospheric and Solar-Terrestrial Physics*, **doi:10.1016/j.jastp.2008.11.011**, Article in press, (2009a)

[18] J.K. Hargreaves, "Auroral absorption of HF radio waves in the ionosphere: A review of results from the first decade of riometry", *Proceedings of the IEEE,* **57**, 1348–1373 (1969)

[19] E. C. Stone, A. M. Frandsen, R. A. Mewaldt, E. R. , Christian, D. Margolies, J. F. Ormes, F. Snow. "The Advanced Composition Explorer", *Space Science Reviews*, **86**, Issue 1/4, pp. 1-22 (1998).

[20] J. Buchau, G.J. Gasman, C.P. Pike, R.A. Wagner and J.A. Whalen, "Precipitation patterns in the Arctic ionosphere determined from airborne observations", *Annales de Geophysique*, **28**, 443-453 (1972)

[21] J.D. Whitehead, "Production and prediction of sporadic E", *Review of Geophysical Space Physics*, **8**, 1, 65-144 (1970)

[22] J.A Whalen, J. Buchau and R.A. Wagner, "Airborne ionospheric and optical measurements of noontime aurora", *Journal of Atmospheric and Terrestrial Physics*, **33**, 661 (1971)

[23] R.A. Wagner, A. L. Snyder and S. -I. Akasofu, "The structure of the polar ionosphere during exceptionally quiet periods", *Planetary and Space Science*, **21**, 11, 1911-1916 (1973)

[24] N. Naridner, I. Steen Mikkelsen and T. Stockflet Jørgensen, "On the formation of high latitude Es-layers", *Journal of Atmospheric and Terrestrial Physics*, **42,** 841 – 852 (1980)

[25] S.E.Ritchie, and F. Honary, "Case studies of enhanced E-layer formation at high-latitudes following Sudden Commencement Absorption events", *The 10th IET international conference on Ionospheric Radio Systems and Techniques*, 18-21 July, London, UK (2006)

[26] W.R. Piggott, K. Rawer, "URSI handbook of ionogram interpretation and reduction", 2nd Edition, Report UAG-23, World Data Centre A for solar terrestrial physics, NOAA, Boulder, Colorado, (1972)

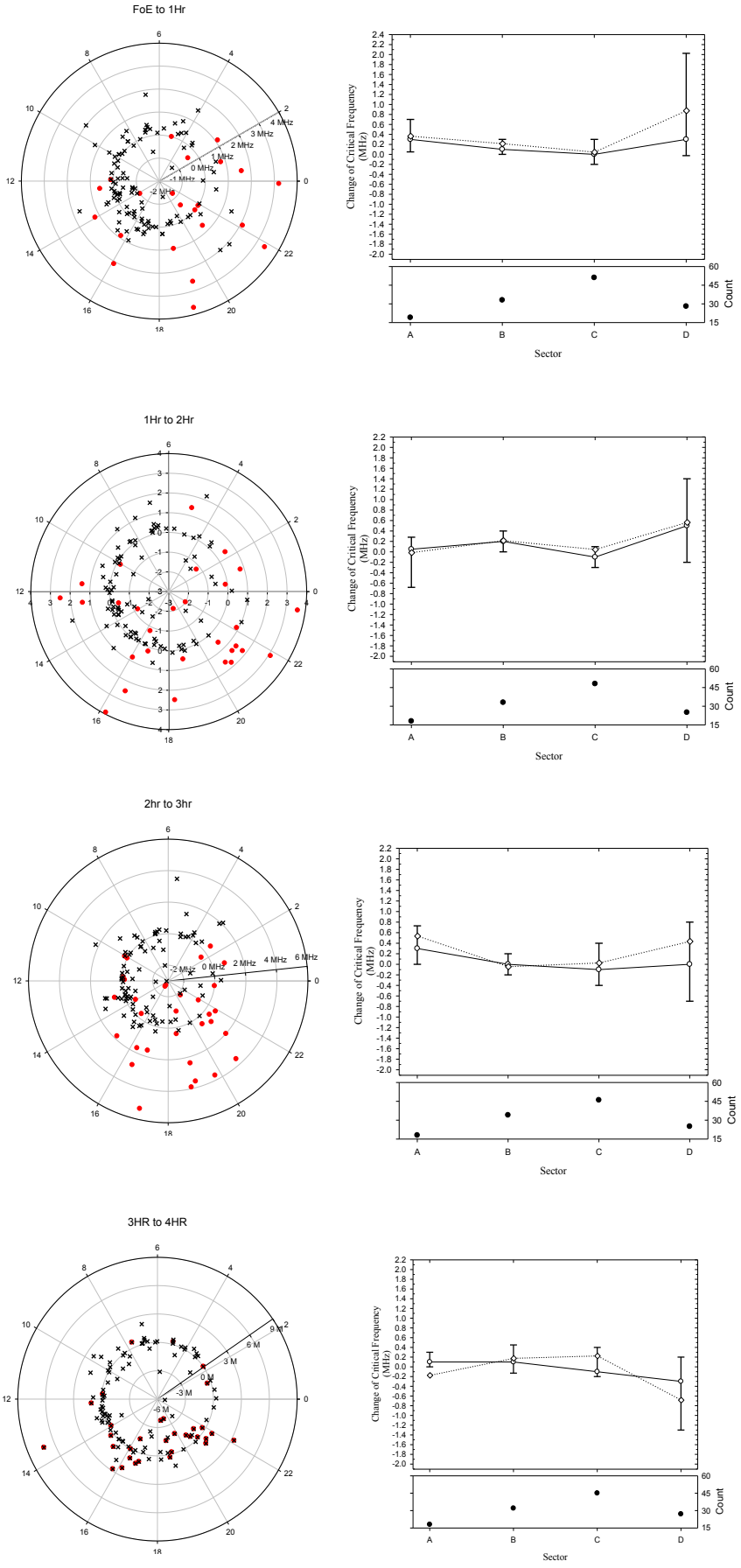

Figure 4 Polar plot – the radial axis is Δf_oE and the clock hours indicate local time. The solid dots indicate where full screening of the F layers occurred. The associated line, scatter and error bar plot shows the mean (diamond) and median (circles) values of Δf_oE_{m-n} per sector, the 25% and 75% percentiles between vertical error bars and the count of events in the lower panel.